

# Influence of Variable Particle Size Reinforcement on Mechanical and Wear Properties of Alumina Reinforced 2014Al Alloy Particulate Composite

**Bharath V**

Research Scholar  
Department of Mechanical Engineering  
Siddaganga Institute of Technology, Tumkur  
Visvesvaraya Technological University  
Belagavi, Karnataka  
India

**Ashita D H**

PG Scholar  
Department of Mechanical Engineering  
Siddaganga Institute of Technology, Tumkur  
Visvesvaraya Technological University  
Belagavi, Karnataka  
India

**V Auradi**

Associate Professor  
Department of Mechanical Engineering  
Siddaganga Institute of Technology, Tumkur  
Visvesvaraya Technological University  
Belagavi, Karnataka  
India

**Madeva Nagaral**

Deputy Manager  
Aircraft Research Design Center HAL  
Bengaluru, Karnataka  
India

*Al<sub>2</sub>O<sub>3</sub> may be the most important reinforcement in aluminum-based composites that are rising quickly in modern years. The significance of this paper is to study the influence of Al<sub>2</sub>O<sub>3p</sub> size variation (i.e. 53 μm and 88 μm) and content (i.e. 9, 12, and 15Wt %) on density, hardness, tensile strength, elongation to fracture and wear studies. During the preparation of each composite, the ceramic reinforcements were introduced in a novel way which involves two-stage additions of reinforcements during liquid stirring. It has been found that because the size of the Al<sub>2</sub>O<sub>3p</sub> is reduced, measurement of the density showed that 2014Al-Al<sub>2</sub>O<sub>3p</sub> composites contained slight porosity and also the quantity of porosity among the prepared composites higher with diminishing the Al<sub>2</sub>O<sub>3p</sub> size and increasing weight percentage of Al<sub>2</sub>O<sub>3p</sub>. In addition to this, the results show that by decreasing the Al<sub>2</sub>O<sub>3p</sub> size and increasing the weight proportion of the Al<sub>2</sub>O<sub>3p</sub> the tensile strength and hardness of the prepared composites increase. Microstructural characterization carried out for the 2014Al-Al<sub>2</sub>O<sub>3</sub> composites using scanning electron microscopy (SEM) which showed a fairly homogeneous distribution of Al<sub>2</sub>O<sub>3p</sub> with grain refinement of the matrix. Wear test is conducted for the prepared composites by utilizing a computerized pin on disc wear testing machine which shows greater wear resistance property as the size of the Al<sub>2</sub>O<sub>3p</sub> reduced.*

**Keywords:** Particulate Metal Matrix Composites (PMMCs); Particle size; Scanning Electron Microscopy (SEM); Mechanical properties; Wear Rate.

## 1. INTRODUCTION

Aluminium Particulate Metal Matrix Composites (PMMC's) have a significant involvement to the advancement technology for the wide range of applications. This is because of their high quality and rigidity to weight proportion and the ability to function at comparatively high temperatures compared with the metal matrix while retaining isotropic properties. Among metal alloys, aluminum combinations are the most prominent in shaping metal matrix composites because of their low density, high thermal conductivity, and versatility in production. PMMC's variety of options involves efficiency driven advanced aviation systems and price sensitive automotive components such as rotor blades, connecting rod crank shafts, camshafts, carden shafts, propeller for helicopters and components of engine for example, cylinders and chamber liners and [1-5] in moderately elevated temperature applications. Since the aluminum-based PMMC is manufactured utilizing a pliable metal as the matrix and ceramic (SiC or Al<sub>2</sub>O<sub>3</sub>) as fortification this outcome is a blend of high-resistance, hardness, and modulus of elasticity along

with great flexibility and durability of the composite [6-10].

Aluminum combinations are widely recognized for their high strength to weight proportion contrasted with several other commercially viable metal composites. However this additional benefit reduces at elevated temperatures ( $\geq 250^{\circ}\text{C}$ ) because of their moderately low dissolving temperature. Utilizing ceramic particle reinforcement, for example, SiC or Al<sub>2</sub>O<sub>3</sub>, to shape aluminum composites gives quality improvement at increased temperature without losing a economic benefits. In addition, by increasing the composite volume fraction of the reinforcement, the ultimate strength at room temperature and at elevated temperature has also been demonstrated [6, 9-11]. The level of progress in the composite properties enormously relies upon the natural properties of both reinforcement and matrix, the homogeneous dispersion of the reinforcement, and its size and volume proportion, bonding strength between the constituents at the interface. Researchers have reported issues identified with PMMC prompting wide disperse in a definitive strength and malleability due to non-homogeneity of the strengthening of the reinforcing particle dispersion [11-13].

The micro-sized ceramic particle has been effectively used to produce aluminum PMMC's through various methods, for example, powder metallurgy [14], fluid metal infiltration [15], compo-casting [16] and squeeze casting [17]. Among these, stir casting is the most

Received: April 2020, Accepted: June 2020

Correspondence to: Bharath V, Research Scholar of Mechanical Engineering, Siddaganga Institute of Technology, Visvesvaraya Technological University, Belagavi, India. Email: bharathv88@gmail.com

doi:10.5937/fme2004968B

© Faculty of Mechanical Engineering, Belgrade. All rights reserved

FME Transactions (2020) 48, 968-978 968

encouraging one for integrating discontinuous reinforcement scattered aluminum metal matrix composites as a result of its better matrix-particle bonding, simpler control of matrix structure, effortlessness, and ease of handling, closer net shape and the wide choice of materials with all shape casting process [18]. In addition, reduction of strengthening particles size results in enhancement of composite quality [19]. One more benefits of reducing reinforcing particles is improved machinability of PMMC's particles, for example, SiC and Al<sub>2</sub>O<sub>3</sub> reason for speed up wear of the machining instruments. From the literature survey, it is seen that small data is accessible as respects the mechanical and wear properties of 2014Al reinforced with Al<sub>2</sub>O<sub>3</sub> particulates MMC's processed by two-stage stir casting route. With an increase in demand for advanced materials in the promising modern applications, where Al-based composites are being considered as a contender to supplant steel or aluminum alloys. Classic examples are liners and round and hollow leaders of the vehicle motors, just as brake rotors.

Keeping the above perceptions in see, it has been proposed to create 2014Al-Al<sub>2</sub>O<sub>3p</sub> composites by varying the Al<sub>2</sub>O<sub>3p</sub> content (i.e. 9, 12, and 15 Wt. %) and size variation (i.e. 53 μm and 88 μm) by two-stage stir casting method. During processing, Al<sub>2</sub>O<sub>3p</sub> particles were added to molten Al in the step of two i.e. entire mass of particles were divided into two equal parts before preheating and added into the vortex of the melt at 750°C to avoid aggregation of particles in Al matrix. It has been intended to study the impact of Al<sub>2</sub>O<sub>3p</sub> content and size variation on the properties include density, hardness, tensile strength, elongation to fracture, and wear studies of 2014Al-Al<sub>2</sub>O<sub>3p</sub> composites developed by stir casting method.

## 2. MATERIAL PREPARATION

In the present study 2014Al alloy (Al-4.0Cu-0.7Si-0.83Mn-0.19Zn-0.63Mg-0.27Fe-0.01Cr-0.06Ti), Al<sub>2</sub>O<sub>3p</sub> is used as matrix and reinforcement respectively. Stir casting method was adopted to prepare 2014Al-Al<sub>2</sub>O<sub>3p</sub> metal matrix composites by varying the particle size (53 and 88μm) and weight percentage (9, 12, and 15wt %) of Al<sub>2</sub>O<sub>3p</sub>. By using an electrical resistance furnace the calculated amount of 2014Al alloy which is placed in a graphite crucible is heated to a temperature of 750<sup>0</sup>C. Once this temperature achieved solid hexachloroethane (C<sub>2</sub>Cl<sub>6</sub>) is introduced into the melt for effective degassing, later the preheated (at a temperature of 250<sup>0</sup>C) Al<sub>2</sub>O<sub>3p</sub> were added into the vortex of the liquefied alloy. With the help of a steel impeller coated with zirconia, the vortex is generated and the impeller speed was maintained at 400 RPM. The molten composite was poured at a temperature of 750°C into the permanent CI (cast iron) mold in the shape of cylinders having a dimension of 12.5mm diameter and 125mm length. Using SEM microstructural examination was carried out for the 2014Al-Al<sub>2</sub>O<sub>3p</sub> composites. The Hardness, tensile measurement of the as-cast 2014Al and 2014Al- Al<sub>2</sub>O<sub>3p</sub> composites were carried out using Z-wick Micro-Vickers hardness and computerized universal tensile testing machine. By using a pin on disc wear testing machine wear properties were evaluated and extents of improvements are noted

down. To reduce the errors, for each test three test specimens were used and the value reported is an average of three tests. Figure 1 shows the permanent mold for producing composites. Molding dies are made of cast iron. For the easy removal of the casting, the dies were made of two halves called split dies which were pin jointed and clamped using C-clamp.



Figure 1. Permanent mold for producing composites.

### 2.1 Microstructure

The composite was produced via a stir casting method, preliminary experiments were first separated to facilitate estimation of the uniform dispersion of Al<sub>2</sub>O<sub>3p</sub>. Later the prepared samples were refined with 400, 800, and 1200 SiC (Silicon carbide) grit papers, individually. In the end, the refined samples were finished on silk cloth the use of a diamond paste of 3 μm. In the same manner, as cast 2014 Al alloy was also refined. With the help of scanning electron microscope (SEM) microscopic examinations were conducted on the as-cast 2014Al alloy and prepared composites.

### 2.2 Density measurement

The density of a composite is received via displacement methods [20] employing a physical balance with a density measurement unit as per ASTM: D792 test approach. Due to the distinction between the theoretical and experimental density of each sample porosity of the prepared composites was examined.

### 2.3 Hardness and tensile tests

As per the ASTM E384 standard, the polished central portion of the casted specimen was taken to measure the micro Vickers hardness of the as-cast 2014Al alloy and prepared composites. The surface of the specimen was produced by grinding via 400, 800, and 1200 SiC (Silicon carbide) grit papers later, specimens were polished with 3 μm diamond paste. To determine the Micro Vickers hardness values of the samples a load of HV 2 is applied for 30 seconds with the help of a diamond cone indenter. The obtained value is the average of 100 readings which is taken at 30 different locations to prevent the segregation effects. For the prepared composites, as per the ASTM E8 standards tensile test was carried out by using a universal testing machine to know the mechanical behavior. Three test samples were utilized for each run. Tensile strength and percentage elongation were extracted with the help of the stress-strain curves.

## 2.4 Wear testing

Wear assessments have been performed by ASTM-G99 standard for the ready composite specimens through a pin on disc wear tester as described in Yasmin et.al. [21]. The pin was once held against the counterface of a rotating EN32 steel disc of 80mm track diameter. By using a deadweight method of loading the pin was loaded opposite to the rotating disc. The dimension of ready composite specimens is 25mm in length and 8mm in diameter. Using a SiC emery paper of 200 grit size, the surface of the ready composite specimen was polished to confirm the effectual flat surface contact with the rotating disc, For each test before and after weighing, the wear track and the ready composite specimen were cleaned by using acetone. Test samples are weighed on analytical balance with accuracy of 0.01mg, before and after each test to calculate weight loss. The wear loss is calculated by weight loss in grams reported during each test and the obtained value is the average of three readings. Using calculated value of the densities of the test sample the weight loss is converted to volume loss. During the experiment a sliding speed of 1.256 m/sec, a sliding distance of 3600m, and a constant load of 29.43N (0.58MPa) have been steady all during the experiment.

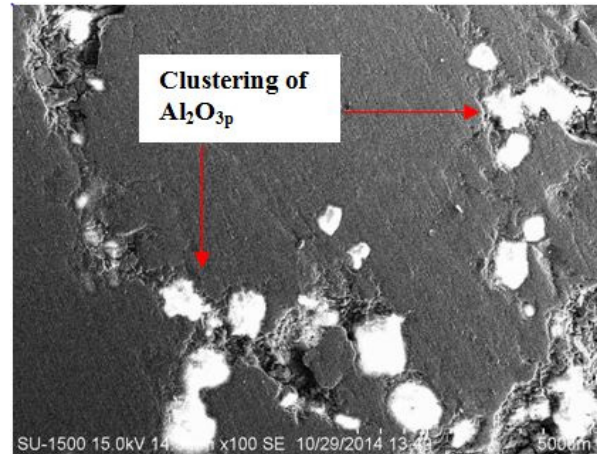
## 3. RESULTS AND DISCUSSION

### 3.1 Microstructure

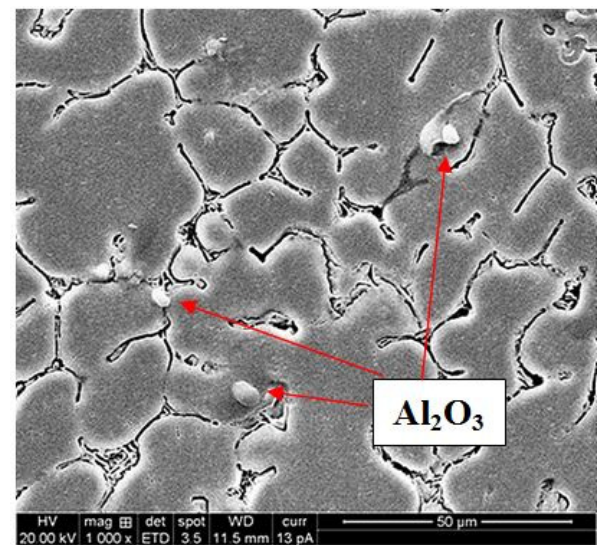
SEM images of 2014Al- $\text{Al}_2\text{O}_3$  (9, 12, and 15 wt %) reinforced composites with 53  $\mu\text{m}$  and 88 $\mu\text{m}$  particle size were produced by stir casting are revealed in Figure 2. The main intention in the preparation of 2014Al- $\text{Al}_2\text{O}_3$  composites is to achieve uniform distribution of  $\text{Al}_2\text{O}_3$ . The uniform dispersion of reinforcing particles obtained in the prepared composite is the result of two-stage stirring. Since the entire weight of the reinforcing particles is added in two steps which ensures homogeneous dispersion overcoming the viscosity difference.

As revealed in figure 2(a-c) and figure 3(a-c), uniform distribution of the  $\text{Al}_2\text{O}_3$  was accomplished in the composites reinforced with 53 $\mu\text{m}$  and 88 $\mu\text{m}$   $\text{Al}_2\text{O}_3$ . Figure 2(b-c) reveals the SEM images of the clustering and agglomeration of the 12 and 15wt. % of  $\text{Al}_2\text{O}_3$  (i.e. for 88 $\mu\text{m}$  particle size) probably because as the wt.% of reinforcement increases, clustering increases due to an increase in surface energy, and bond is weakened between the hard ceramic and soft matrix thereby decreasing wettability [22]. However, agglomerations in some areas were observed due to the porosities present [23]. Figure 3(a-c) reveals the uniform distribution of 53 $\mu\text{m}$   $\text{Al}_2\text{O}_3$ , whereas in Figure 2(a-c) distribution of 88 $\mu\text{m}$  particles was not that much uniform compared to 53  $\mu\text{m}$  particles, and some of these particles are agglomerated. Accordingly, SEM perceptions of the microstructures reveal that the distribution of 53 $\mu\text{m}$  size  $\text{Al}_2\text{O}_3$  was progressively uniform, while the 88 $\mu\text{m}$  size  $\text{Al}_2\text{O}_3$  leads to the segregation and agglomeration of  $\text{Al}_2\text{O}_3$ . The probable reason for the segregation of  $\text{Al}_2\text{O}_3$  can be given as that during solidification, solidification of the dendrites occurs at first and then surplus particles are moved and clustered at inter-dendritic regions using the

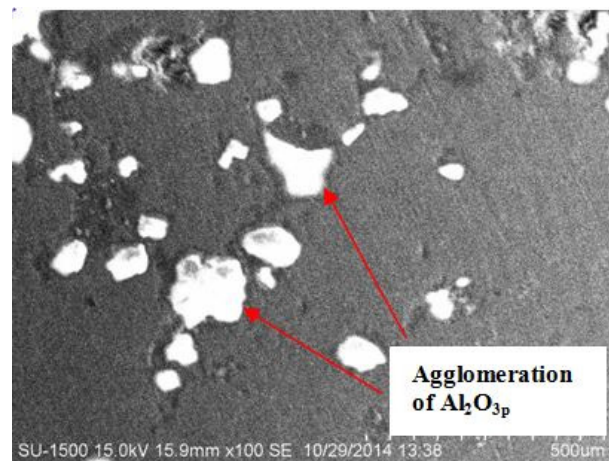
solid-liquid interface. Segregation of the particles is more effective with finer particles [24].



2 (a)



2 (b)



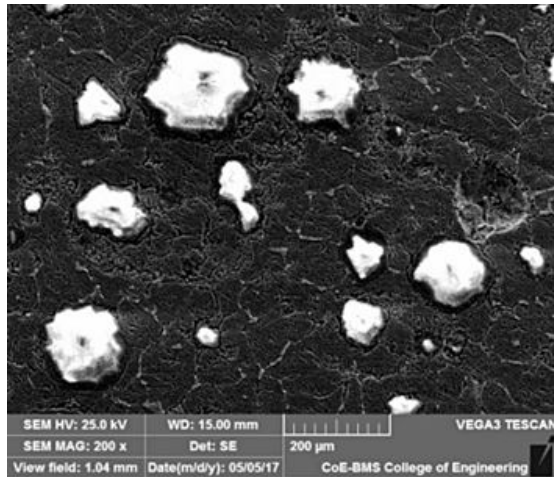
2 (c)

Figure 2 (a-c) SEM images of 2014Al- $\text{Al}_2\text{O}_3$  composites at different wt% of  $\text{Al}_2\text{O}_3$  content (9, 12, and 15 wt. %) with a particle size of 88 $\mu\text{m}$ .

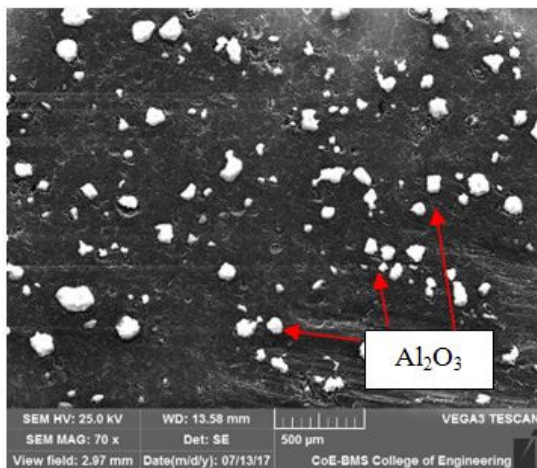
The actual amount of elements present in the predefined zone of the sample is revealed by energy dispersive spectroscopy. Figure 4(a) and figure 4(b) demonstrate the outcomes of the energy dispersive spectroscopy for 2014Al reinforced with 12 wt. % of  $\text{Al}_2\text{O}_3$  for different particle size (i.e. 88 $\mu\text{m}$  and 53 $\mu\text{m}$ ) which contains oxide and aluminum this confirms the presence of  $\text{Al}_2\text{O}_3$ .

**Table.1 The Theoretical, Experimental, Micro-hardness, UTS, and % Elongation of 2014Al alloy and its composites reinforced with 9-15wt%  $Al_2O_3p$  and variable particle size**

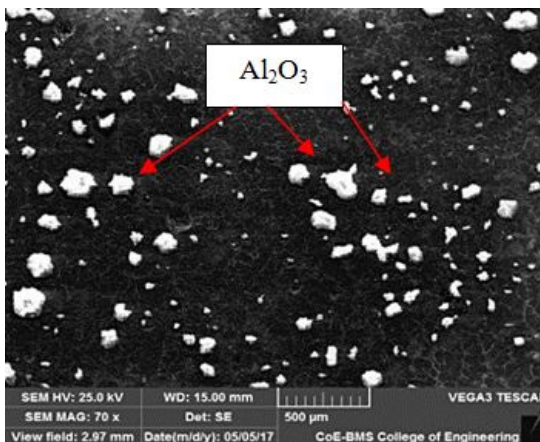
Samples	Particle Size	Theoretical Density ( $g/cm^3$ )	Experimental Density ( $g/cm^3$ )	Microhardness (HV)	UTS (MPa)	Percentage Elongation (%)
2014Al	-	2.80	2.78±0.01	99 ± 2.63	149.29 ± 4.53	4.51 ± 0.24
9Wt. % $Al_2O_{3p}$ /2014Al	88 $\mu$ m	2.87	2.7±0.01	104.7 ± 5.52	167.9 ± 4.16	3.95 ± 0.17
12Wt. % $Al_2O_{3p}$ /2014Al		2.89	2.75±0.01	142.27 ± 1.36	173.61 ± 3.56	2.93 ± 0.12
15Wt. % $Al_2O_{3p}$ /2014Al		2.91	2.81±0.02	167.25 ± 5.20	193.47 ± 2.87	2.24 ± 0.13
9Wt. % $Al_2O_{3p}$ /2014Al	53 $\mu$ m	2.87	2.57±0.01	127.89 ± 6.83	184.69 ± 4.45	3.11 ± 0.34
12Wt. % $Al_2O_{3p}$ /2014Al		2.89	2.59±0.02	149.8 ± 1.45	206.75 ± 4.89	2.53 ± 0.53
15Wt. % $Al_2O_{3p}$ /2014Al		2.91	2.65±0.02	183.02 ± 6.50	226.76 ± 5.98	1.56 ± 0.17



3 (a)



3 (b)



3 (c)

Figure 3 (a-c) reveals the SEM images of 2014Al- $Al_2O_{3p}$  composites at different wt% of  $Al_2O_{3p}$  content (9, 12, and 15 wt. %) with a particle size of 53 $\mu$ m.

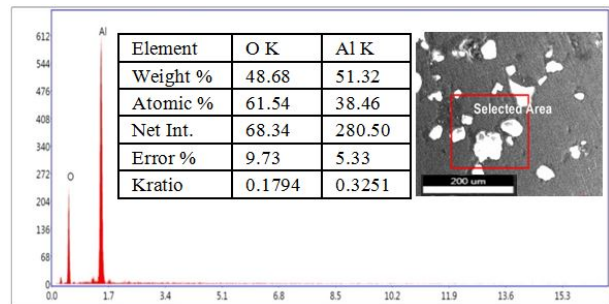


Figure 4 (a) EDS outcome of 2014Al alloy with 12 wt. %  $Al_2O_{3p}$  (88 $\mu$ m)

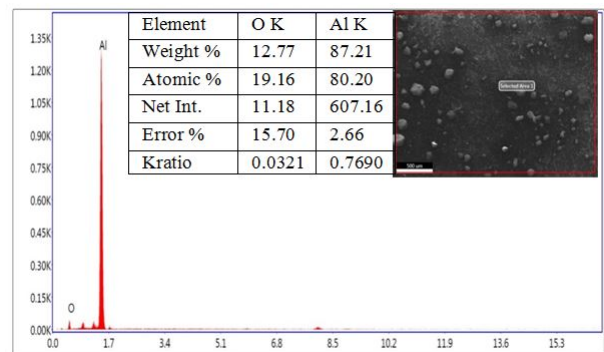


Figure 4 (b) EDS outcome of 2014Al alloy with 12 wt. %  $Al_2O_{3p}$  (53 $\mu$ m)

### 3.2 Density and porosity measurement

Experimental and theoretical densities and porosities of 2014Al alloy reinforced with different particle sizes (i.e. 53 and 88 $\mu$ m  $Al_2O_{3p}$ ) at different weight fractions (i.e. 9, 12 and 15Wt %) of  $Al_2O_{3p}$  are illustrated in figure 5 and figure 6 individually and corresponding density values are given in Table.1. By using the rule of mixture theoretical densities are calculated in which the results show there a linear increase value of above-prepared composites. In the meantime, experimental densities values were accomplished by experimentation for 9, 12, and 15 wt. % of  $Al_2O_{3p}$  (53 $\mu$ m and 88 $\mu$ m) composites. Densities of the composites were determined by experimentally by utilizing sample mass and dimensions [25].

From figure 5 it can be concluded that the values obtained for the experimental density are lesser than the values of the theoretical density, which could be the after effect of porosity developed during composite fabrication. Throughout the production method of the MMCs, some porosity is likely a direct result of the steady in surface area, in contact with air, due to the entrapment of the gas while casting, hydrogen pro-

gression, appropriate pouring distance between the mold and the crucible and shrinkage throughout solidification [26]. Likewise decrease in the density of the composite got in the present work is in great concurrence with prior work by Mohanty et. al. [27].

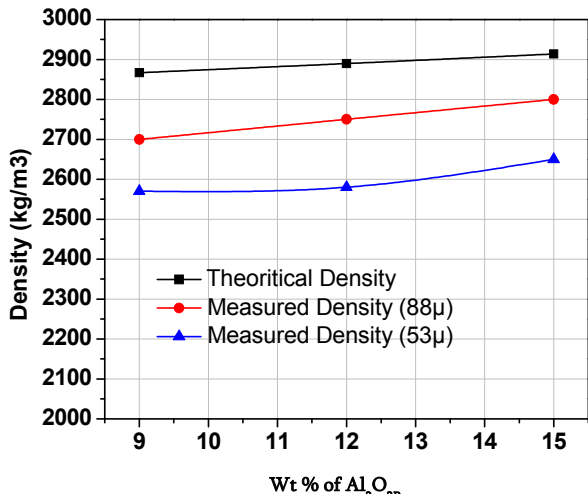


Figure 5. Graphical representation of theoretical and experimental density with different wt% of Al<sub>2</sub>O<sub>3p</sub> (9, 12, and 15 wt. %) content and size (53µm and 88µm).

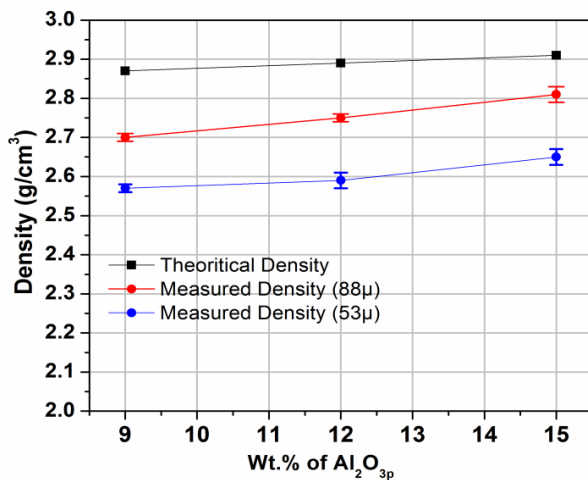


Figure 6. Graphical representation porosity with different wt% of Al<sub>2</sub>O<sub>3p</sub> (9, 12, and 15 wt. %) content and size (53µm and 88µm).

Figure 6 shows the graphical representation of porosities of the prepared composites i.e. 2014Al alloy reinforced with different particle sizes (i.e. 53 and 88µm Al<sub>2</sub>O<sub>3p</sub>) at different weights fractions (i.e. 9, 12 and 15Wt % of Al<sub>2</sub>O<sub>3p</sub>). Meantime for the above-prepared composites, the amount of density and porosity is increased by increasing the weight fraction of Al<sub>2</sub>O<sub>3p</sub>, and decreasing the Al<sub>2</sub>O<sub>3p</sub> size is demonstrated in figure 5 and figure 6. These outcomes have been seen in earlier examinations [28, 29, and 30].

### 3.3 Hardness and tensile test

By utilizing micro Vickers hardness testing machine hardness tests were performed on 2014Al alloy reinforced with different weight fractions (9, 12, and 15 wt. %) of Al<sub>2</sub>O<sub>3p</sub> with a particle size of 53µm and 88µm. The effects of variable particle size during hardness tests are shown in figure 7(a) and obtained

values are given in the table.1 From figure 7(a) it is concluded that as the weight percentage of Al<sub>2</sub>O<sub>3p</sub> increases from 9-15wt% and decreasing the particle size hardness of the above prepared composite increases. This improvement is a direct result of the essence of Al<sub>2</sub>O<sub>3p</sub> [31] in the 2014Al matrix and particulate fortifying of the matrix material. It has been accounted for that the nearness of hard reinforcement particle prompts to plastic twisting during the test [32]. Because of the expansion in strain energy, the hardness of the composite increments at the fringe of the particles scattered in the matrix. The expansion in the hardness of Al<sub>2</sub>O<sub>3p</sub> particles with diminishing the particle size can likewise be ascribed to the uniform dispersion of Al<sub>2</sub>O<sub>3p</sub> in the 2014Al matrix.

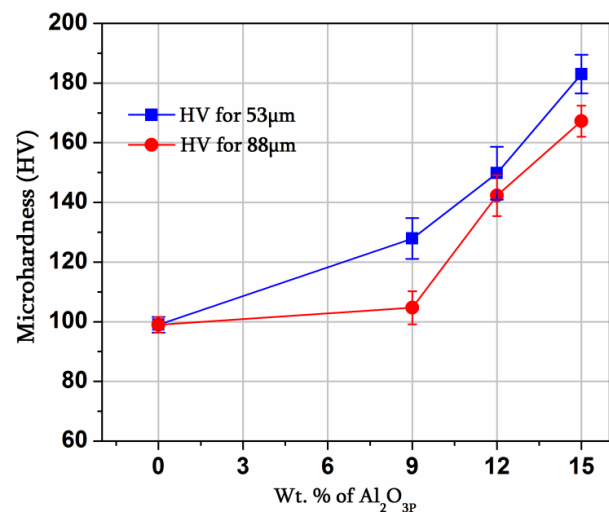
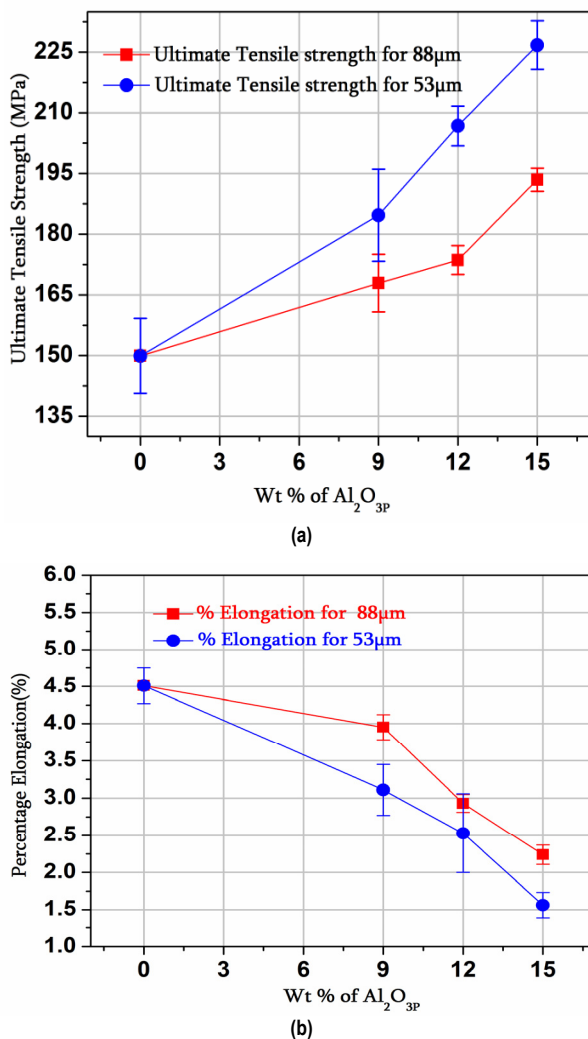


Figure 7 Variation of microhardness for different wt. % of Al<sub>2</sub>O<sub>3p</sub> (0, 9, 12, and 15 wt. %) content and size (53µm and 88µm).

Figure 8a and table.1 shows the results of the tensile test for the 2014Al alloy reinforced with different wt. % (9, 12, and 15 wt. %) of Al<sub>2</sub>O<sub>3p</sub> and with the variation in the particle size of 53µm and 88µm respectively. As shown in figure 8(a) by decreasing the particle size (88µm-53µm) and increasing the weight fraction (%) of Al<sub>2</sub>O<sub>3p</sub> tensile strength of the above-prepared composites increases.

The explanations behind enhancements acquired with Ultimate tensile strength (UTS) is; (i) At the interface between the ceramic particle and the base metal bond respectability is reliant on load move [33]; (ii) During handling of composites there are changes in the microstructure; because of the transfer of the load between the hard ceramic Al<sub>2</sub>O<sub>3p</sub> and ductile matrix 2014Al alloy bringing about fortifying and upgrading tensile strength [33, 34]; (iii) Thermal mismatch between Al matrix (23X10<sup>-6</sup>/°C) and ceramic Al<sub>2</sub>O<sub>3p</sub> (8.2X10<sup>-6</sup>/°C) will bring about increment in dislocation density separated from catching of disengagements in the matrix by second phase ceramic Al<sub>2</sub>O<sub>3p</sub> particles during deformation [35]. From the figure 8(a) it can be concluded that the composite reinforced with 53µm size of the Al<sub>2</sub>O<sub>3p</sub> with different weight fraction (9, 12 and 15 wt. %) shows a greater result than that of the composite reinforced with 88µm size of the Al<sub>2</sub>O<sub>3p</sub> (9, 12 and 15 wt. %).



**Figure 8. (a-b) Variation of the tensile strength and percentage elongation with different wt. % of Al<sub>2</sub>O<sub>3p</sub> content (0, 9, 12, and 15 wt. %) and size (53µm and 88µm) respectively.**

The calculated elongation for above-prepared composites lies with an extremely low range, less than 5%, rely on the Al<sub>2</sub>O<sub>3p</sub> content and size. As an increase in particle content and a decrease in particle size, lower will be the elongation is shown in figure 8(b). The decrease in extension is clear as ceramic reinforcement is having lower flexibility in examination with the matrix and during tensile loading, the unformed Al<sub>2</sub>O<sub>3</sub> particle could cause pressure focus around the particles. Consequently, particles collected at grain limits intensified the pressure focuses.

Hardness and tensile strength of the prepared composites are higher as compared to as-cast 2014 Al alloy, and by adding Al<sub>2</sub>O<sub>3p</sub> the hardness and tensile strength of the Al alloy increases [29, 35].

It is concluded that with the above-prepared composites, high tensile strength and higher hardness and minimum elongation are observed in composites with a particle size of 53µm.

### 3.4 Wear test

Figure 9(a-b) illustrates the outcome of wear rate as a feature of sliding distance for as-cast 2014 Al alloy strengthened with 0, 9, 12, and 15 wt. % Al<sub>2</sub>O<sub>3p</sub> with a

variable particle size of 88µm and 53µm respectively. Sliding speed is adjusted to 1.256 m/sec, a diameter of the wear track is 80mm and a load 29.43N (0.58MPa).

Figure 9(a-b) shows that the wear rate increases at the initial stage, which could be due to the adhesive nature of wear at the initial phase [36, 37]. Once the initial transition period (run in wear) is over, the materials wear rate falls and a steady-state value of wear rate are achieved. Moreover, the steady-state wear approaches for the composites (2014Al-9,12 and 15 wt. % Al<sub>2</sub>O<sub>3p</sub>) with a variable particle size (88 and 53µm) at nearly 3000m sliding distance and run-in wear approaches for the composite (2014Al-9,12 and 15 wt.% Al<sub>2</sub>O<sub>3p</sub>) with a particle size of 88µm is higher as compared to the composite (2014Al-9,12 and 15 wt.% Al<sub>2</sub>O<sub>3p</sub>) with a particle size of 53µm at all sliding distance as shown in Fig. 9(a) and (b). However, with the increase in the sliding distance from 600m to 3600m, the wear rate of composite decreases as compare to the as cast 2014Al matrix alloy. Figure 9(a-b) illustrates lesser wear rate of the composites (2014Al-9, 12 and 15 wt. % Al<sub>2</sub>O<sub>3p</sub>) with a variable particle size of 88 and 53µm as compared to base alloy (2014Al). This is owing to the fact that the inclusion of hard ceramic Al<sub>2</sub>O<sub>3p</sub> in 2014 Al alloy prevents such plowing action of hard steel counterpart and thereby MMCs wear resistance increases.

Figure 9(a) shows the MMCs (2014Al-Al<sub>2</sub>O<sub>3p</sub>) with a particle size of 88µm shows the excessive wear rate and this will be attributed to the weak surface strength between the base alloy and 88µm size Al<sub>2</sub>O<sub>3p</sub> at a different weight percentage (9, 12 and 15wt %) as an outcome of the little contact surface zone. These conditions facilitate an increase in the wear rate due to the particle pull out from the base alloy. Also, MMCs (2014Al-Al<sub>2</sub>O<sub>3p</sub>) with a particle size of 53µm exhibits a lower wear rate compared to the MMCs containing a particle size of 88µm owing to the enhancement of the load-bearing ability of the 53µm particle size compare to the 88µm particle size.

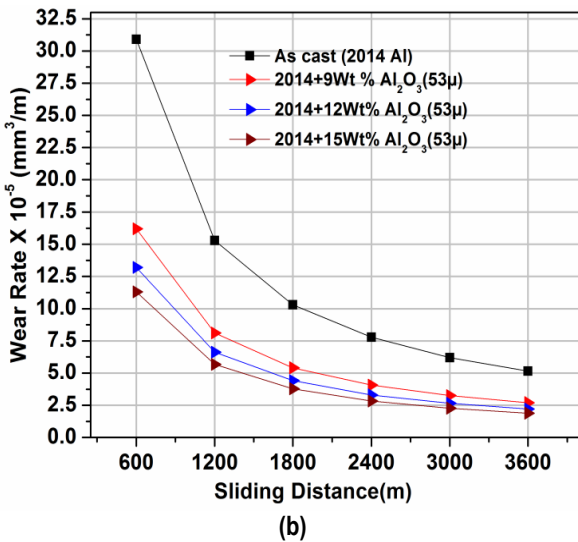
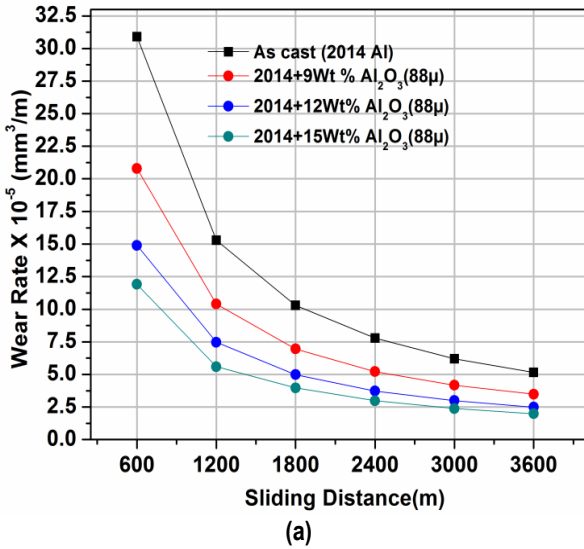
more interfacial strength exists between the 2014Al matrix alloy and 53µm size Al<sub>2</sub>O<sub>3p</sub> owing to the great surface bonding which makes it hard for the particle pullout from the 2014Al matrix. Hence, it is concluded that an increase in weight percentage (9, 12, and 15wt %) and a decrease in the Al<sub>2</sub>O<sub>3p</sub> size which provides reduced wear rate, thereby wear resistance of the MMCs increases.

Figure 10 shows an almost gradual increase in the volume loss with the increase in the sliding distance took place for as-cast 2014 Al alloy strengthened with 0, 9, 12, and 15wt. % Al<sub>2</sub>O<sub>3p</sub> with a variable particle size of 88µm and 53µm at a constant load of 29.43N (0.58MPa) and 1.256 m/sec sliding speed for a distance of 3600m. The standard deviation of volumetric wear loss values of the produced composites are shown in Table 2.

Figure 10 determines the appropriate comparative wear curves formed and duration of running-in and onset of steady state period. The wear curves represented in Figure 10 were formed by measuring the mass of the test specimens at the outset of the test and at each time in testing (after 600, 1200, 1800, 2400, 3000 and 3600 m), so the volumetric wear loss was calculated for the above stated sliding distances.

**Table.2 Standard deviation of volumetric wear loss for 2014Al alloy and its composites reinforced with 9-15wt% Al<sub>2</sub>O<sub>3p</sub> and variable particle size.**

Samples	Particle Size	Sliding Distance(m)					
		600	1200	1800	2400	3000	3600
		Volumetric wear loss (cm <sup>3</sup> )					
2014Al	-	0.09 ± 0.006	0.18 ± 0.010	0.23 ± 0.038	0.35 ± 0.050	0.46 ± 0.036	0.55 ± 0.025
9Wt. % Al <sub>2</sub> O <sub>3p</sub> /2014Al	88μm	0.11 ± 0.012	0.15 ± 0.010	0.22 ± 0.015	0.34 ± 0.021	0.42 ± 0.010	0.49 ± 0.010
12Wt. % Al <sub>2</sub> O <sub>3p</sub> /2014Al		0.10 ± 0.021	0.15 ± 0.015	0.22 ± 0.021	0.30 ± 0.015	0.39 ± 0.012	0.45 ± 0.031
15Wt. % Al <sub>2</sub> O <sub>3p</sub> /2014Al		0.05 ± 0.015	0.11 ± 0.017	0.16 ± 0.012	0.29 ± 0.015	0.38 ± 0.015	0.47 ± 0.021
9Wt. % Al <sub>2</sub> O <sub>3p</sub> /2014Al	53μm	0.10 ± 0.021	0.17 ± 0.031	0.21 ± 0.025	0.24 ± 0.020	0.27 ± 0.036	0.28 ± 0.029
12Wt. % Al <sub>2</sub> O <sub>3p</sub> /2014Al		0.07 ± 0.015	0.12 ± 0.020	0.14 ± 0.021	0.20 ± 0.030	0.22 ± 0.032	0.25 ± 0.021
15Wt. % Al <sub>2</sub> O <sub>3p</sub> /2014Al		0.07 ± 0.015	0.11 ± 0.021	0.15 ± 0.010	0.19 ± 0.015	0.21 ± 0.029	0.22 ± 0.026



**Figure 9 (a-b) Variation of wear rate against the sliding distance of the composite (2014Al- 9, 12, and 15 wt. % Al<sub>2</sub>O<sub>3p</sub>) (a) 88μm and (b) 53μm Al<sub>2</sub>O<sub>3p</sub> particle reinforced.**

The as cast 2014 Al alloy and varying weight percentage of Al<sub>2</sub>O<sub>3</sub> particulates reinforced composites wear curves show two different slopes, which relates the initial (running-in) period and the steady-state period, i.e. before the onset of the typically lower and linear steady-state wear, running-in wear appears as the initial high-rate transient wear, same was observed by Aleksandar Vencl et al. [38] for A356 alloy reinforced with SiC and graphite particulates. In the present study wear curves (figure 10) shows running in period upto 2400m and from 2400 to 3600m shows steady state period.

From figure 10 it is observed that the volumetric wear loss increases in 2014Al matrix alloy as the sliding distance increases and similar trends are seen in the case of the composite with different particle sizes (88-53μm).

Further, it is observed that as the reinforced particle size decreased from 88-53μm, the volume loss of the composites gets reduced as contrasted to the 2014Al matrix alloy. i.e., the wear resistance increases with increasing in wt. % of Al<sub>2</sub>O<sub>3p</sub> (9-15 wt.%) and decreasing the particle size (88-53μm). Overall, figure 10 reveals that the volumetric wear loss increases initially and thereafter remains insensitive to sliding distance. Similar observations were made by other researchers Basavarajappa et al. [39]. Zhang et al. [40] examine the wear behavior of the composites.

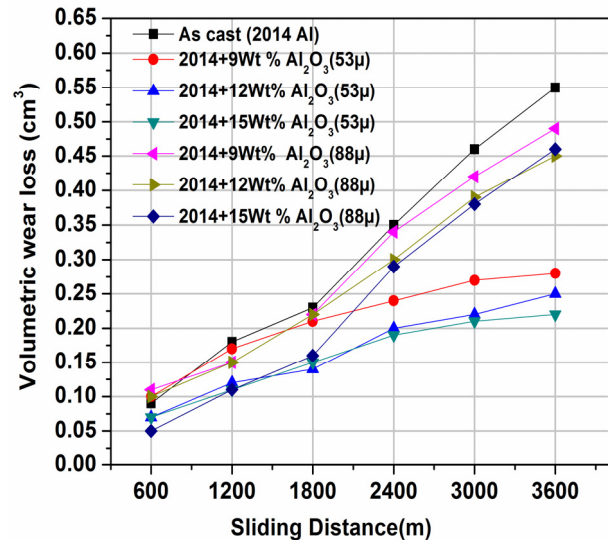


**Figure 10 Volumetric wear loss as a function of sliding distance at 29.43N constant load and 300 rpm sliding speed**

### 3.5 Worn surface studies

As cast 2014Al alloy and produced composites (2014 Al-Al<sub>2</sub>O<sub>3p</sub>) worn surface SEM images for different particle size are demonstrated in figure 11(a-e). From the SEM images it is found that somehow worn surface morphology of produced composites is distinct from that of the as-cast matrix alloy (figure.11.a). The as-cast 2014Al matrix alloy demonstrated clear plastic flow of material on the sample contact surface, while for composites (2014Al-9 and 15 wt. % Al<sub>2</sub>O<sub>3</sub>) with a particle size of 88μm, it was barely noticeable, and for composite (2014Al-9 and 15 wt. % Al<sub>2</sub>O<sub>3</sub>) with a particle size of 53μm, it couldn't have been identified at all. 2014Al alloy matrix (figure.11.a) shows the deep

and larger grooves on the surface and also increases the thickness and width of the grooves, while fine grooves are observed in case of  $88\mu\text{m}$   $\text{Al}_2\text{O}_3\text{p}$  composite (figure 11.b-c) and this type of morphologies are very less in case of  $53\mu\text{m}$   $\text{Al}_2\text{O}_3\text{p}$  composite produced (figure 11.d-e) which indicates that the composite reinforced with  $53\mu\text{m}$   $\text{Al}_2\text{O}_3\text{p}$  has an enhanced capacity to withstand maximum load as the sliding distance increases during wear testing.

Figure 11(d-e) demonstrates SEM images of produced composites (2014Al-9 and 15 wt. %  $\text{Al}_2\text{O}_3$ ) with a particle size of  $53\mu\text{m}$   $\text{Al}_2\text{O}_3\text{p}$  and it is observed that, at all sliding distance the produced composites results in smooth and thin surfaces as contrasted to 2014Al alloy matrix and composite produced with a particle size of  $88\mu\text{m}$ . Figure 11(d-e) the produced composites with  $53\mu\text{m}$  lead to lower extent of damage as contrasted to as-cast 2014Al matrix alloy and composite produced with  $88\mu\text{m}$ . Possible reason for this matrix alloy results in lower surface strength contrasted to composite produced and is quickly softened by the generated heat at the interface. In the present study, both the matrix and produced composite with  $88\mu\text{m}$   $\text{Al}_2\text{O}_3\text{p}$  results in severe damage as compared to the composite produced with  $53\mu\text{m}$   $\text{Al}_2\text{O}_3\text{p}$  and it can be distinctly observed from the worn surfaces SEM images.

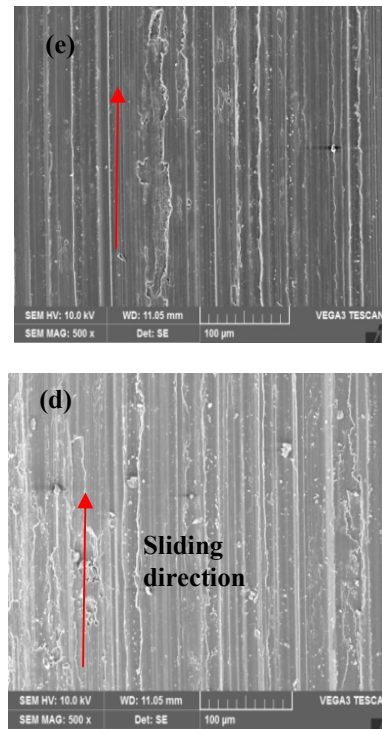
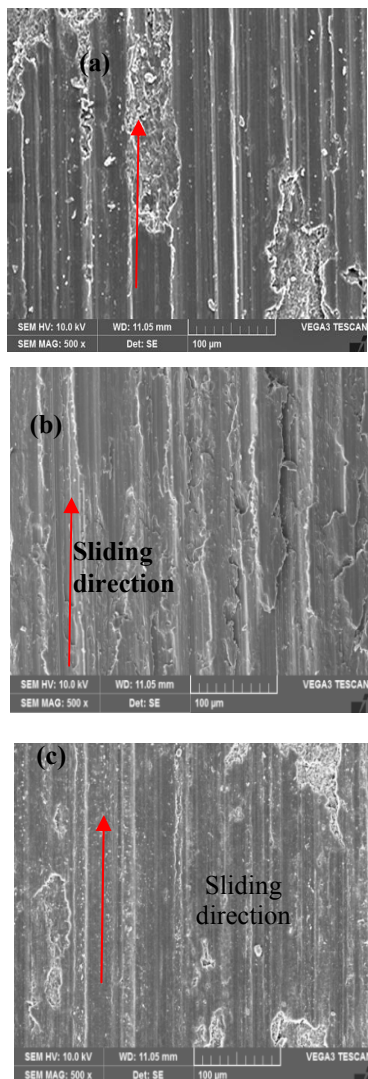


**Figure.11 (a-e) Worn surface images, (a) as-cast 2014Al alloy, (b-c) and (d-e) 2014Al-9 and 15 wt. %  $\text{Al}_2\text{O}_3\text{p}$  with a particle size of  $88\mu\text{m}$  and  $53\mu\text{m}$  respectively.**

#### 4. CONCLUSIONS

2014Al alloy reinforced with  $\text{Al}_2\text{O}_3\text{p}$  is mainly used in the field of aerospace and automobile, to be more specific it is used in building the structural frame for aerospace vehicles. Their properties like physical and mechanical properties like high hardness, low density, high electrical conductivity, etc., can be enhanced with the addition of ceramic materials as reinforcements; this present work is also such an attempt to enhance and to know the impact of variable particle size reinforcement on mechanical and wear properties of 2014Al- $\text{Al}_2\text{O}_3\text{p}$  composite has led to following conclusions:

1. 2014Al- $\text{Al}_2\text{O}_3\text{p}$  MMC's with different weight percentage and variable particle size have been effectively synthesized by stir casting method.
2. Microstructural studies revealed that 2014Al- $\text{Al}_2\text{O}_3$  MMCs with the particle size of  $53\mu\text{m}$  have a better distribution of  $\text{Al}_2\text{O}_3\text{p}$  in comparison to the particle size of  $88\mu\text{m}$  wherein lead to agglomeration and isolation of  $\text{Al}_2\text{O}_3\text{p}$  were observed.
3. The density and porosity of the 2014Al- $\text{Al}_2\text{O}_3$  MMC's increased with an increase in weight percentage (9-15wt %) and decreasing the particle size.
4. 2014Al- $\text{Al}_2\text{O}_3$  MMC's have shown improvement in hardness for 0, 9, 12, and 15wt%  $\text{Al}_2\text{O}_3\text{p}$  and also with decreasing the particle size.
5. The tensile strength of 2014Al- $\text{Al}_2\text{O}_3$  MMCs increased with an increase in the weight percentage (9-15wt %) and decreasing the particle size but the elongation of them decreased.
6. With an increase in weight percentage and decreasing the particle size, wear results indicate the decreasing trend of wear rate, and thereby improves the wear resistance.

7. In the present study,  $Al_2O_3$  of  $53\mu m$  and  $88\mu m$  have been utilized. This can additionally be stretched out to other particle sizes to study the effect of particle size on mechanical and wear properties and also the prepared composite can subject to heat-treatment and then mechanical properties and wear properties shall be evaluated at different varying parameters like load, sliding time, sliding distances, etc. Even work can be conducted in extreme atmospheric conditions and wet sliding conditions shall also be used.

#### ACKNOWLEDGMENT

The authors are thankful for the Organizing chair, Guest Editor, Department of Mechanical Engineering, CMR Technical Campus of the First International Conference on Advanced Lightweight Materials and Structures – ICALMS-2K20, Hyderabad, India for permitting to publish this work

#### REFERENCES

- [1] S. C. Tung, M.L. McMillan.: Automotive Tribology overview of current advances and challenges for the future, *Tribology International*, Vol. 37, pp 517-536, 2004. DOI:10.1016/j.triboint.2004.01.013
- [2] S. Das.: Development of aluminum alloy composites for engineering applications, *Transactions of Indian Institute of Metals*, Vol. 57, No. 4, pp 325-334, 2004.
- [3] A Vencl, A Rac and I Bobic.: Tribological Behaviour of Al-Based MMC's and their applications in Automotive Industry. *Tribology in Industry*, Vol.26 (3-4), 2004.
- [4] A. Vencl. Tribology of the Al-Si Alloy Based MMCs and their application in Automotive Industry, in: L. Magagnin (Ed.), *Engineered Metal Matrix Composites: Forming Methods, Material Properties and Industrial Applications*, Nova Science Publishers, New York, USA, 2012, pp.127–166.
- [5] Sandra Veličković, Slobodan Garić, Blaža Stojanović, and Aleksandar Vencl. Tribological properties of aluminium matrix nanocomposites, *Applied Engineering Letters*, 1, 3, 2016, 72-79.
- [6] Khaled A. Al-Dheylyan, Amro Al-Qutub, and Syed Hafeez "Tensile Response of Aluminum Reinforced with Submicron  $Al_2O_3$  Metal Matrix Composites" *Proceedings of the International Conference on Recent Advances in Mechanical and Materials Engineering*, Kuala Lumpur, Malaysia Paper No. 52. May 2005.
- [7] V. C. Nardone and K. M. Prewo.: On the Strength of Discontinuous Silicon Carbide Reinforced Aluminum Composites, *Scripta Metallurgica*, Vol.20(1),43-48,1986. [https://doi.org/10.1016/0036-9748\(86\)90210-3](https://doi.org/10.1016/0036-9748(86)90210-3)
- [8] B. G. Park, A. G. Crosky and A. K. Hellier.: Fracture Behavior and Toughness of and Al 6061 Metal Matrix Composites, *Journal of Australasian Ceramic Society*, Vol.30 (1-2), pp 41-47. 1994.
- [9] K. R. Suresh, H. B. Niranjana, P. Martin Jebaraj, and M. P. Chowdiah.: Tensile and Wear properties of Aluminum Composites, *Wear*, Vol.255 pp 638-642, 2003. [https://doi.org/10.1016/S0043-1648\(03\)00292-8](https://doi.org/10.1016/S0043-1648(03)00292-8).
- [10]Majid Hoseini and Mohamood Mertian.: Tensile Properties of in-situ Aluminum-Alumina Composites, *Materials Letters*, Vol.59, pp.3414-3418. 2005.
- [11]L. Ceschini, G. Minak, and A. Morri.: Tensile and Fatigue Properties of the AA6061/20 vol.%  $Al_2O_3$  and AA7005/10 vol.%  $Al_2O_3$  Composites, *Composites Science and Technology*, Vol.66, pp. 333-342, 2006. <https://doi.org/10.1016/j.compscitech.2005.04.044>
- [12] T. J. A. Doel and P. Bowen.: Tensile Properties of Particulate Reinforced Metal Matrix Composites, *Composites Part A*, Vol.27A, pp 655-665, 1996. [https://doi.org/10.1016/1359-835X\(96\)00040-1](https://doi.org/10.1016/1359-835X(96)00040-1)
- [13]S. J. Hong, H. M. Kim, D. Huh, C. Suryanarayana, and B. S. Chun.: Effects of Clustering on the Mechanical Properties of SiC Particulate-Reinforced Aluminum Alloy 2024 Metal Matrix Composites, *Material Science and Engineering Vol.A347*, pp 198-204, 2003.
- [14]A. M. Al-Qutub, I.M. Allam, and T.W. Qureshi: Wear Properties of 10% Sub-Micron  $Al_2O_3$  / 6061 Aluminum Alloy Composite, *International Journal of Applied Mechanics and Engineering*, Vol.7, pp.329-334, 2002.
- [15]M. Kouzeli, and D. C. Dunand.: Effect of Reinforcement Connectivity on the Elasto-Plastic Behavior of Aluminum Composites Containing Sub-Micron Alumina Particles, *ActaMaterialia*, Vol. 51 pp. 6105-6121, 2003. [https://doi.org/10.1016/S1359-6454\(03\)00431-2](https://doi.org/10.1016/S1359-6454(03)00431-2)
- [16]M Kočić, A Vencl, I Bobic, M Ristic, M Antic, Z Milutinovic.: Joining of composite materials based on Al-Si alloys by using the GMAW process. *Welding and Material Testing*, 23, 3, pp.9-12, 2014.
- [17]Xiufang Wang, Gaohui Wu, Dongli Sun, Changjiu Qin, and YunglongTian.: Micro-Yield Property of Sub-Micron  $Al_2O_3$  Particle Reinforced 2024 Aluminum Matrix Composite, *Materials Letters*, Vol.58, pp. 333-336, 2004.
- [18]S. Ray.: Review: Synthesis of cast metal matrix particulate composites, *Journal of Material Science*, vol. 28, pp 5397-5413, 1993.
- [19]Paul S. Gilman "Discontinuously Reinforced Aluminum: Ready for the 1990s, *Journal of Metals*, pp.7-15, 1991.
- [20]B.K. Prasad.: Investigation into sliding wear performance of zinc-based alloy reinforced with SiC particles in dry and lubricated conditions, *Wear*, Vol. 262, pp. 262–273, 2007. <https://doi.org/10.1016/j.wear.2006.05.004>
- [21]Yasmin T, Khalid AA, Haque M. Tribological (wear) properties of aluminum-silicon eutectic base alloy under dry sliding condition, *Journal of Materials Processing Technology*, Vol. 153–154,

pp.833–838.2004.

DOI:10.1016/j.jmatprotec.2004.04.147

- [22] M. Kok.: Production and mechanical properties of  $Al_2O_3$  particle-reinforced 2024 aluminum alloy composites Journal of materials processing technology, Vol.161, issue.3, pp.381-387, 2005, <https://doi.org/10.1016/j.jmatprotec.2004.07.068>
- [23] S.P. Chaudhary, P.K. Singh, S. Rai, H. Patel, Bharat Kumar. : A Review on Effect of Reinforcement Particles on the Mechanical Properties of Aluminium Based Composites, International Journal of Innovative Research in Science, Engineering and Technology, Vol. 4, Issue 9, pp.8377-8382, 2015
- [24] McCoy, O.W. and Franklin, E.W.: Dendritic Segregation in Particle-Reinforced Cast Aluminum Composites. In: Fishman, S.G. and Dhingra, A.K., Eds., Proceedings of the International Symposium on Advances in Cast Reinforced Metal Composites, ASM International Publications, Materials Park, pp.237-242, 1988.
- [25] M.D. Bermudez, G. Martinez-Nicolas, F.J. Carrion, I. Martinez-Mateo, J.A. Rodriguez, and E.J. Herrera.: Dry and lubricated wear resistance of mechanically-alloyed aluminum-base sintered composites, Wear, Vol. 248 pp. 178–186, 2001. [http://dx.doi.org/10.1016/S0043-1648\(00\)00553-6](http://dx.doi.org/10.1016/S0043-1648(00)00553-6)
- [26] J. Hashim, L. Looney, and M.S.J. Hashmi.: Metal Matrix Composite: Produced by Stir Casting Process, Journal of Materials Processing Technology, Vol. 92, pp. 1–7, 1999.
- [27] R. M Mohanty, K Balasubramaniam, S. K. Seshadri.: Boron carbide-reinforced aluminum 1100 matrix composites: Fabrication and properties, Materials science, and Engineering. A vol. 498, pp. 42, 2008 DOI:10.1016/j.msea.2007.11.154
- [28] G.S. Hanumanth, G.A. Irons.: Particle incorporation by melt stirring for the production of metal-matrix composites, Journal of Material Science, vol.28, pp. 2459–2465, 1993. <https://doi.org/10.1007/BF01151680>
- [29] M. Kok.: Production of Metal Matrix ( $Al_2O_3$ -reinforced) Composite Materials and Investigation of Their Machinability by Ceramic Tools, Ph.D. Thesis, Firat University, Elazığ, Turkey, 2000.
- [30] P.K. Ghost, S. Ray.: Influence of process parameters on the porosity content in Al(Mg)-alumina cast particulate composite produced by Vortex method, AFS Transaction, 775 (782), pp.88–214, 1988.
- [31] P. Mittal, Gajendra Dixit.: Dry Sliding Wear Behaviour of 2014 Aluminium Alloy Reinforced with Sic Composite, International Journal of Engineering Research & Technology, Vol.5, pp.147-153, 2016.
- [32] V. Bharath, Madeva Nagral, V. Auradi, S.A. Kori.: Preparation of 6061Al- $Al_2O_3$  MMC's by stir casting and evaluation of mechanical and wear properties, Procedia Material Science, vol.6, pp. 1658-1667, 2014. <https://doi.org/10.1016/j.mspro.2014.07.151>
- [33] V.S. Gaharwar, V. Umashankar.: The characterization and behavior of Al2014 reinforced with  $Al_2O_3$  fabricated by powder metallurgy, International Journal of Chemical Technology Research, vol.6, pp. 3272-3275, 2014
- [34] O.P. Modi, Two-body abrasion of a cast Al–Cu (2014 Al) alloy– $Al_2O_3$  particle composite: influence of heat treatment and abrasion test parameters, Wear, Vol. 248, pp.100-111, 2001. [https://doi.org/10.1016/S0043-1648\(00\)00534-2](https://doi.org/10.1016/S0043-1648(00)00534-2)
- [35] K.Purazrang, P. Abachi, K.U. Kainer.: Investigation of the mechanical behavior of magnesium composites, Composites, Vol. 25 (4), pp. 296–302, 1994
- [36] Chaudhary, S. K., A. K. Singh, C. S. Sivaramakrishnan, and S. C. Panigrahi. 2005. Wear and friction behavior of spray formed and stir cast Al-2Mg-11TiO<sub>2</sub> composites. Wear 258:759–767.
- [37] Frey, D., M. B. God, and W. O. Peterson. 1980. Wear Control Handbook, 283–312. New York: ASME.
- [38] Aleksandar Vencl, Filip Vučetić, Biljana Bobić, Ján Pitel and Ilija Bobić.: Tribological characterization in dry sliding conditions of compocasted hybrid A356/SiCp/Grp composites with graphite macroparticles, The International Journal of Advanced Manufacturing Technology, Vol. 11, 9-12, 2019, pp. 2135-2146).
- [39] S. Basavarajappa, G. Chandramohan, Arjun Mahadevan, Mukundan Tangavelu, R. Subramanian, P. Gopalkrishnan.: Influence of the sliding speed on the dry sliding wear behavior and the subsurface deformation on hybrid metal composite, Wear, 262, pp. 1007-1012, 2007, <https://doi.org/10.1016/j.wear.2006.10.016>
- [40] Zhang Mei Juan, CAO Zhan, Yang Xiao Hong, Liu Yong Bing.: Microstructure and wear properties of graphite and  $Al_2O_3$  reinforced AZ1D-Cex composites, Transactions of Nonferrous Metals Society of China, 20, pp. 471-475, 2010.

---

**УТИЦАЈ ПРОМЕНЉИВЕ ВЕЛИЧИНЕ  
ЧЕСТИЦА НА МЕХАНИЧКЕ И КАРАКТЕ-  
РИСТИКЕ ХАБАЊА КОМПОЗИТА НА БАЗИ  
АЛУМИНИЈУМА ОЈАЧАНОГ ЧЕСТИЦАМА  
ЛЕГУРЕ 2014А1**

**Барат В., Ашита Д.Х., В. Ауради, М. Нагарал**

У новије време  $Al_2O_3$  се највише користи за ојачавање композита на бази алуминијума. Рад истражује утицај варирања величине  $Al_2O_{3p}$  (53  $\mu m$  - 88 $\mu m$ ) и садржаја (9, 12, 15 Wt %) честица на густину материјала. У току припремања сваког композита увођено је керамичко ојачање новим поступком, који се састоји од двофазног додавања ојачања за време мешања течного материјала. Утврђено је да услед редуковања величине честица  $Al_2O_{3p}$  густина композита 2014Al- $Al_2O_{3p}$  има малу порозност и да је већа када опада величина честица  $Al_2O_{3p}$  и расте тежински проценат  $Al_2O_{3p}$ . Резултати такође показују да се повећава затезна чврстоћа и

тврдоћа са опадањем величина честица и порастом тежинског процента. Карактеризација микроструктуре је извршена применом SEM технике. Утврђена је знатна дистрибуција хомогености  $Al_2O_{3p}$  са

пречишћеним честицама у матрици. Испитивање отпорности на хабање извршено је на pin-on-disk машини. Отпорност на хабање расте са опадањем величина честица  $Al_2O_{3p}$ .